

First-Order Character and Observable Signatures of Topological Quantum Phase Transitions

A. Amaricci,¹ J. C. Budich,^{2,3} M. Capone,¹ B. Trauzettel,⁴ and G. Sangiovanni⁴

¹*Democritos National Simulation Center, Consiglio Nazionale delle Ricerche, Istituto Officina dei Materiali (IOM) and Scuola Internazionale Superiore di Studi Avanzati (SISSA), Via Bonomea 265, 34136 Trieste, Italy*

²*Institute for Theoretical Physics, University of Innsbruck, 6020 Innsbruck, Austria*

³*Institute for Quantum Optics and Quantum Information, Austrian Academy of Sciences, 6020 Innsbruck, Austria*

⁴*Institut für Theoretische Physik und Astrophysik, Universität Würzburg, Am Hubland, D-97074 Würzburg, Germany*

(Received 5 December 2014; revised manuscript received 17 March 2015; published 8 May 2015)

Topological quantum phase transitions are characterized by changes in global topological invariants. These invariants classify many-body systems beyond the conventional paradigm of local order parameters describing spontaneous symmetry breaking. For noninteracting electrons, it is well understood that such transitions are continuous and always accompanied by a gap closing in the energy spectrum, given that the symmetries protecting the topological phase are maintained. Here, we demonstrate that a sufficiently strong electron-electron interaction can fundamentally change the situation: we discover a topological quantum phase transition of first-order character in the genuine thermodynamic sense that occurs without a gap closing. Our theoretical study reveals the existence of a quantum critical endpoint associated with an orbital instability on the transition line between a 2D topological insulator and a trivial band insulator. Remarkably, this phenomenon entails unambiguous signatures related to the orbital occupations that can be detected experimentally.

DOI: [10.1103/PhysRevLett.114.185701](https://doi.org/10.1103/PhysRevLett.114.185701)

PACS numbers: 64.70.Tg, 05.30.Rt, 71.10.Fd, 71.30.+h

Introduction.—The advent of topological insulators [1–3] has given a surprising twist to the venerable topic of band structure physics: Triggered by the theoretical prediction [4–6] and experimental observation [7] of the quantum spin Hall effect, topological aspects of band insulators and superconductors have become one of the most active research fields in physics, culminating in a new periodic table [8–10] that exhaustively lists all topologically distinct band structures in the ten Altland-Zirnbauer symmetry classes [11]. For the integer quantum Hall effect, the archetype of a topological state, the discovery of the striking quantization of a natural response quantity, namely, the Hall conductance [12], preceded its theoretical explanation in terms of topology [13,14]. In contrast, most of the topological invariants of the periodic table are not directly related to bulk observables. The identification of experimentally detectable signs of topological states and of phase transitions between them is hence an open challenge.

In conventional Landau-Ginzburg theory, different states of matter are classified by spontaneous symmetry breaking, associated with local order parameters. Phase transitions of this kind are generically of first order; i.e., the order parameter and other relevant observables display discontinuities at the phase boundary, providing us with a natural way of detecting them [15]. On the contrary, topological phase transitions elude this paradigm as they are associated with a change in global invariants. Since in the noninteracting case, the band structure evolves continuously

as a function of the control parameters, topological transitions are always continuous and accompanied by a closure of the energy gap, given that the protecting symmetries are preserved and that the Hamiltonian is short ranged. The inclusion of strong electronic correlations may however lead to new scenarios [16–24]. In this regard, a natural and still open question is whether correlation-induced topological transitions can exhibit novel experimental signatures, compared to their noninteracting analogs.

Here, we report for the first time the occurrence of a *first-order* topological quantum phase transition in a microscopic model. In a sense, strong correlations add to the topological transition a thermodynamic first-order behavior, even though the phase transition is not associated to the onset of any conventional long-range order. This allows us to identify natural experimental fingerprints of the topological transition, in addition to the global invariants. Specifically, by solving a two-orbital Hubbard model with dynamical mean-field theory (DMFT), we show that a transition between a band insulator (BI) and a quantum spin Hall insulator (QSHI) takes place without the continuous closing of the band gap in the electronic spectrum if the Coulomb repulsion is large enough. In this strongly correlated regime, the interaction-induced QSHI is thus in proximity to a first-order transition line and to a quantum critical endpoint associated with a correlation-driven criticality in the orbital channel. A direct, yet crucial, implication of this result is the

identification of a critical behavior in measurable quantities related to the orbital polarization.

Model.—We study a minimal two band Fermi-Hubbard model with both inter- and intraband interactions on a two-dimensional square lattice exhibiting the quantum spin Hall effect [25]. The model Hamiltonian reads as

$$\mathcal{H} = \sum_{\mathbf{k}} \psi_{\mathbf{k}}^\dagger \hat{\mathbf{H}}_0(\mathbf{k}) \psi_{\mathbf{k}} + \sum_i \mathcal{H}_{\text{int}}(i),$$

$$\mathcal{H}_{\text{int}}(i) = (U - J) \frac{N_i(N_i - 1)}{2} - J \left(\frac{N_i^2}{4} + S_{zi}^2 - 2T_{zi}^2 \right) \quad (1)$$

where $\psi_{\mathbf{k}} = (c_{1\mathbf{k}\uparrow} \ c_{2\mathbf{k}\uparrow} \ c_{1\mathbf{k}\downarrow} \ c_{2\mathbf{k}\downarrow})$ and the operator $c_{\mathbf{k}\alpha\sigma}^\dagger$ ($c_{\mathbf{k}\alpha\sigma}$) creates (annihilates) an electron in orbital $\alpha = 1, 2$ with momentum \mathbf{k} and spin σ . N_i is the number operator for the electrons on site i , summed over α and σ . S_{zi} and T_{zi} are the z components of the total spin S_i and orbital pseudospin T_i operators, respectively. When referring to the local components of these operators, we will drop the subscript i . The local orbital polarization, e.g., will therefore read $T_z = (n_{1\uparrow} + n_{1\downarrow} - n_{2\uparrow} - n_{2\downarrow})/2 = (n_1 - n_2)/2$.

The noninteracting part $\hat{\mathbf{H}}_0$ of the Hamiltonian [Eq. (1)] conserves S_z , i.e., it has a $U(1)$ spin rotation symmetry and, hence, is block diagonal in spin: $\hat{\mathbf{H}}_0(\mathbf{k}) = \text{Diag}[\hat{h}(\mathbf{k}), \hat{h}^*(-\mathbf{k})]$. The relation between the two blocks is imposed by time reversal symmetry (TRS). Denoting the orbital pseudospin by τ , the individual blocks have the form $\hat{h}(\mathbf{k}) = d_{\mathbf{k}}^i \tau_i$, with $d_{\mathbf{k}}^x = \lambda \sin(k_x)$, $d_{\mathbf{k}}^y = \lambda \sin(k_y)$, $d_{\mathbf{k}}^z = M - \cos(k_x) - \cos(k_y)$, describing a system of two bands of width $W = 4$ in our units of energy, coupled with an interorbital hybridization λ and separated by an energy splitting $2M$. We set $\lambda = 0.3$ and we have checked that our results are qualitatively robust against this choice. We consider an average density of two electrons per site (half-filling), which corresponds to setting the chemical potential μ at the center of the gap.

In the absence of interaction and with the interpretation of $\alpha = 1, 2$ as orbitals in a semiconductor quantum well, a similar model was originally introduced [6] for HgTe-CdTe heterostructures where the quantum spin Hall effect was first experimentally observed [7]. In our model the two orbitals should be regarded as localized electron wave functions of strongly correlated systems or as lowest Wannier functions in a deep optical lattice with fermionic atoms. The second term \mathcal{H}_{int} in Eq. (1) describes the screened local Coulomb repulsion experienced by the fermions [26]. This term includes both inter- and intra-orbital interaction terms as well as the Hund's coupling J , in order to account for the natural tendency of the interacting electrons to maximize the total spin.

A nonperturbative solution of our interacting model [Eq. (1)] in the thermodynamic limit is attainable by means of DMFT [27]. This approximation goes beyond the

static mean-field (Hartree-Fock) level because it treats the self-energy, which describes all interaction effects entering the single-particle Greens function, as a frequency dependent, though purely local, quantity. The orbital structure, crucial to describe many-body effects on topology [28], is also fully captured within DMFT. Here, the self-energy in the orbital pseudospin space has the form $\hat{\Sigma}(\omega) = \Sigma(\omega)\tau_z$, where $\Sigma(\omega)$ is a scalar complex function. The real part of $\hat{\Sigma}$ at $\omega = 0$ normalizes the energy splitting between the two orbitals: $2M_{\text{eff}} = 2M + \text{Tr}[\tau_z \hat{\Sigma}(\omega = 0)]$.

Results.—The zero temperature paramagnetic phase diagram of our model [Eq. (1)] is shown in Fig. 1(a) in the $1/M$ vs $1/U$ plane. At each point of this diagram, we use a color code proportional to $\Xi = 2[\Sigma(0) - \Sigma(\infty)]$. This quantity measures the deviation of the DMFT self-energy at low frequency from the high-frequency values, which essentially corresponds to the static Hartree-Fock mean field. In other words Ξ quantifies the strength of quantum fluctuations beyond the static mean field or the degree of correlation.

At $U = 0$ we recover the conventional topological transition where the gap closes at $M = 2$, separating the trivial BI from the QSHI. When the interactions U and J are switched on, the two phases undergo a different evolution. The BI, with two electrons in the lower-lying orbital, is essentially unaffected by the interactions, while the QSHI, in which the two orbitals are more equally occupied, is much more exposed to correlation effects. The interactions favor equal population of the orbitals. Therefore, the self-energy correction to $2M$ reduces the energy separation between them [29] and a larger value of M is required to turn the QSHI into a trivial BI. The QSHI-BI transition line in the phase diagram is defined as the locus where the effect of U is balanced by an increase of M which is given by the condition $M_{\text{eff}} = 2$. Crossing this line, the topological \mathbb{Z}_2 invariant, evaluated from the single-particle Green's function [30,31], changes from 0 in the BI, to 1 in the QSHI.

However, the nature of the transition dramatically changes from weak to strong interactions. In the small- U regime the transition remains continuous (dotted line) as in the $U = 0$ limit. For larger interactions the evolution between BI and QSHI turns into a discontinuous first-order transition (thick solid line). A quantum critical point (QCP) at $(1/U_c, 1/M_c)$ separates the two regimes. The change in the character of the transition arises from a nontrivial competition between the single-particle term controlled by M and the interaction proportional to U that we can visualize with the help of the quantity Ξ defined above. For small values of U , the interaction essentially behaves like a single-particle term that renormalizes the band structure parameters, well captured within a Hartree-Fock approximation. This means that Ξ is small for both solutions [see green region on both sides of the dotted line in Fig. 1(a)]. Therefore, the compensation between the M and U terms is basically perfect and the transition

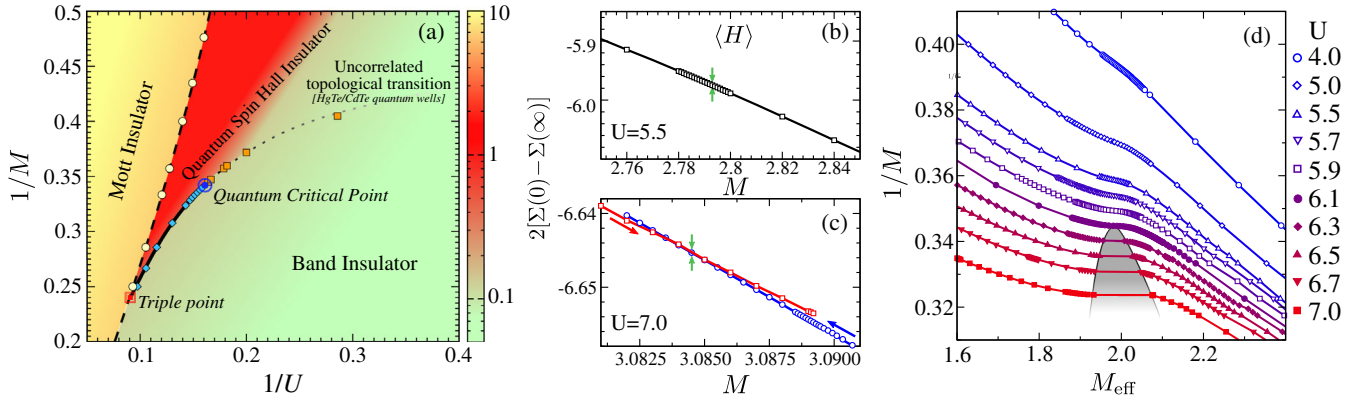


FIG. 1 (color online). (a) $T = 0$ phase diagram in the $1/U$ vs $1/M$ plane for $J = U/4$ and $\lambda = 0.3$. Besides delimiting the different phases—Mott, topological, and band insulator (MI, QSHI, and BI, respectively, in the main text)—the color quantifies the many-body character, as measured by the value of $\Xi = 2[\Sigma(0) - \Sigma(\infty)]$. The orange squares and the dotted line mark the continuous BI-QSHI transition for small U . The blue diamonds and the thick solid line mark the first-order transition between the same phases for large U . The two lines are connected by a quantum critical point. White circles and a dashed line denote the boundary of the MI. (b),(c) Total energy $\langle \mathcal{H} \rangle$ as a function of M , for two values of U . Vertical arrows mark the transition. The red and blue curves in (c) denote the solutions coming from the QSHI and from the BI, respectively. The branches with higher energy correspond to metastable solutions that can be followed beyond the transition point and give rise to hysteresis. (d) Effective band splitting parameter M_{eff} near the quantum critical point showing the critical behavior of the transition.

maintains the properties of the noninteracting system. For larger values of U , higher-order terms of a perturbative expansion must be taken into account. In the framework of DMFT, this is reflected by a significant frequency dependence of the self-energy and an increase of Ξ for the QSHI solution [25], which becomes rapidly more correlated as U increases. On the other hand the BI remains largely unaffected by correlations [see the red region on the QSHI side of the thick solid line, to be contrasted with the BI side remaining green in Fig. 1(a)]. The frequency dependence of the self-energy implies that an increase of the M term can no longer compensate exactly for the dynamical effect of the interactions, and the physical picture is no longer directly linked with the $U = 0$ point. The two ground states cannot be continuously connected and the only way to move from one to the other is a first-order jump. However, the topological characterization of the two phases remains the same as in weak coupling, and in particular the two solutions retain the values of the global topological invariants of their noninteracting counterparts.

The first-order line ends in a triple point, after which U and M are so large that the QSHI solution disappears in favor of a direct transition between the BI and a Mott insulator (MI), which naturally emerges when the interaction strength is larger than any other scale. This highly correlated solution has a high-spin configuration and a very large value of Ξ [yellow in Fig. 1(a)]. We have checked that, releasing the paramagnetic constraint, an antiferromagnet is stable for large U but it does not spoil the critical behavior.

The first-order behavior and the associated hysteresis are further illustrated by the behavior of the internal energy $\langle \mathcal{H} \rangle$ for two interactions, respectively, smaller [panel (b)] and larger [panel (c)] than $U_c = 6.1$. The derivative

$\partial \langle \mathcal{H} \rangle / \partial M \equiv 2 \langle T_z \rangle$ is clearly continuous below U_c and it jumps above U_c , but it does not vanish on either sides of the transition [see Fig. 3(a)], and it cannot be used as an order parameter. On the other hand, the quantity $\Delta M_{\text{eff}} = M_{\text{eff}}(\text{BI}) - M_{\text{eff}}(\text{QSHI})$ calculated *along* the topological transition line, can be viewed as an order parameter. A visual analogy with the liquid-gas transition can be obtained plotting ΔM_{eff} as a function of $1/M$ for different values of U which are the counterparts of the isotherms. The critical behavior is apparent in the corresponding plot of Fig. 1(d). The topological transition in the correlated part of the phase diagram becomes, therefore, of first-order in the usual thermodynamic sense.

Absence of a gap closing.—For noninteracting systems, the topological invariants are defined in terms of integrals over the compact Brillouin zone of functions of the Bloch Hamiltonian, more precisely, of the projection onto its occupied eigenstates. These functions are continuous in all band structure parameters as long as an energy gap is present. As a consequence, if the underlying symmetries of the system are maintained, the discrete-valued topological invariants cannot change without a continuous closing of the energy gap [3,21]. In contrast, by explicit breaking of TRS or particle number conservation [32–34], a QSHI can be connected to a trivial band insulator without a gap closing. In the presence of interactions, the single-particle Green’s function can acquire zeros that are also associated with changes in the topological invariants [35].

Remarkably, the topological quantum phase transition line for $U > U_c$ discovered in this work does not fit into any of the above pictures. The topological transition is of first-order and is accompanied by a discontinuity—in the sense of a finite jump—in the single-particle Green’s

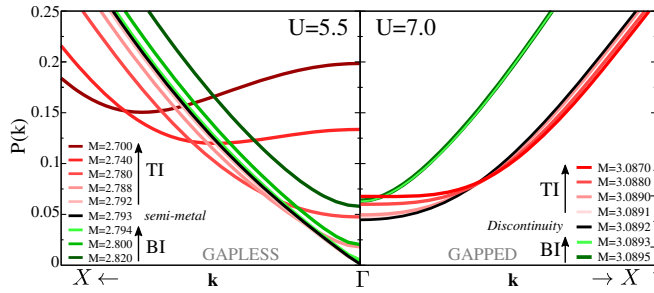


FIG. 2 (color online). Evolution of the poles $P(\mathbf{k})$ (positive part) of the single-particle Green's function near the Γ point across the topological transition for $U = 5.5$ (left panel) and $U = 7.0$ (right panel). At weak interaction (left panel) the transition occurs with a closure of the band gap with the formation of a semimetallic state (Dirac cone). At strong interaction (right panel) the transition takes place without closure of the spectral gap. Here we follow the QSHI solution in its whole existence region.

function. We stress that both TRS and particle number are conserved.

The absence of a gap closing is demonstrated in Fig. 2, in which we compare the evolution of the spectral gap around the Γ point as a function of M for a BI-QSHI transition at $U = 5.5 < U_c$ and at $U = 7.0 > U_c$, respectively. While a Dirac cone at the Γ point is present for $U = 5.5$, the spectrum is gapped for $U = 7.0$. In the latter case the ground state discontinuously jumps from a gapped BI to a gapped QSHI at the first-order transition.

The lack of the zero-gap semimetallic state in the *bulk* electronic structure is a striking dissimilarity between conventional (continuous) and correlation-driven first-order topological transitions. This distinction is, in principle, directly measurable in photoemission experiments [36]. Yet, the thermodynamic characterization of the first-order phase transition for $U > U_c$, enables the identification of natural experimentally detectable differences between the trivial and the nontrivial phase.

Since the QCP discovered here is associated with a critical behavior of M_{eff} , it directly influences the orbital polarization. $\langle T_z \rangle$ indeed changes from a continuous dependence on M , at small U , to a critical one (infinite slope) at U_c and eventually displays a first-order jump beyond the QCP [Fig. 3(a)]. We can quantify this behavior by looking at the orbital compressibility $\kappa = \partial \langle T_z \rangle / \partial M$ [Fig. 3(b)]. κ displays a maximum at the topological transition, which gets sharper upon increasing U and eventually diverges at the QCP. The divergence of the orbital compressibility is an ideal marker of the thermodynamic distinction between the BI and correlated QSHI.

We can identify specific signatures of the interaction-induced topological phase transition also in the spin sector. Unlike conventional band insulators, Mott systems are characterized by the presence of (instantaneous) local magnetic moments and by a Curie-like ($\propto 1/T$) local spin

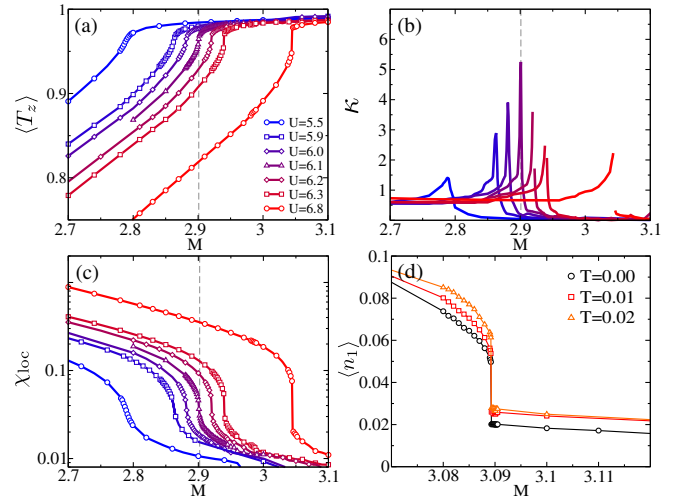


FIG. 3 (color online). First-order character of the topological quantum phase transition in the strongly correlated regime. (a) Local orbital polarization $\langle T_z \rangle$, (b) orbital compressibility $\kappa = \partial \langle T_z \rangle / \partial M$ and (c) local spin susceptibility χ_{loc} as a function M . (d) Temperature dependence of the jump in the orbital occupation of the first (higher-lying) orbital.

susceptibility $\chi_{\text{loc}} = \int d\tau \langle T_\tau S_z(\tau) S_z(0) \rangle$. Remarkably the characteristic critical behavior shows up also in this response function, displayed in Fig. 3(c).

At last, we demonstrate that the first-order character of the topological transition for $U > U_c$ persists at finite temperatures. As reported in Fig. 3(d), the orbital occupation changes slightly with T but the jump remains visible. The discontinuity is therefore resilient to temperatures of the order of the topological gap, which is set by the hybridization λ .

Conclusions.—We have given strong evidence that, in the presence of strong electronic correlations, the topological phase transition from a trivial BI to a QSHI acquires a first-order thermodynamic character. The immediate consequence of this is the presence of a well-defined critical behavior of simple bulk quantities such as the orbital compressibility and the local spin susceptibility. Finally, the analogy with liquid-gas transition suggests a possible strategy to design and realize a correlation-induced QSHI. Let us consider a heterostructure of a MI and a noninverted, i.e., trivial, BI. Because of the proximity to the Mott region, the BI layers close to the interface can increase their correlation strength [37], leading to a decrease of the effective mass term. Near the first-order line this can eventually trigger a discontinuous topological transition of such few layers.

We thank F. Assaad, M. Fabrizio, M. Punk, P. Thunström, and A. Toschi for useful discussions. A. A. and M. C. are supported by the European Union under FP7 ERC Starting Grant No. 240524 “SUPERBAD.” G. S. acknowledges financial support by the Deutsche

Forschungsgemeinschaft through FOR 1346 and FOR 1162, J. C. B. from the ERC Synergy Grant “UQUAM” and B. T. from the DFG-JST research unit “Topotronics,” the DFG priority program SPP1666, the Helmholtz Foundation (VITI), and the ENB graduate school on “Topological Insulators”.

-
- [1] M. Z. Hasan and C. L. Kane, *Rev. Mod. Phys.* **82**, 3045 (2010).
- [2] J. E. Moore, *Nature (London)* **464**, 194 (2010).
- [3] X.-L. Qi and S.-C. Zhang, *Rev. Mod. Phys.* **83**, 1057 (2011).
- [4] C. L. Kane and E. J. Mele, *Phys. Rev. Lett.* **95**, 226801 (2005).
- [5] C. L. Kane and E. J. Mele, *Phys. Rev. Lett.* **95**, 146802 (2005).
- [6] B. A. Bernevig, T. L. Hughes, and S.-C. Zhang, *Science* **314**, 1757 (2006).
- [7] M. König, S. Wiedmann, C. Brüne, A. Roth, H. Buhmann, L. W. Molenkamp, X.-L. Qi, and S.-C. Zhang, *Science* **318**, 766 (2007).
- [8] A. P. Schnyder, S. Ryu, A. Furusaki, and A. W. W. Ludwig, *Phys. Rev. B* **78**, 195125 (2008).
- [9] A. Kitaev, *AIP Conf. Proc.* **1134**, 22 (2009).
- [10] S. Ryu, A. P. Schnyder, A. Furusaki, and A. W. W. Ludwig, *New J. Phys.* **12**, 065010 (2010).
- [11] A. Altland, and M. R. Zirnbauer, *Phys. Rev. B* **55**, 1142 (1997).
- [12] K. v. Klitzing, G. Dorda, and M. Pepper, *Phys. Rev. Lett.* **45**, 494 (1980).
- [13] R. B. Laughlin, *Phys. Rev. B* **23**, 5632 (1981).
- [14] D. J. Thouless, M. Kohmoto, M. P. Nightingale, and M. den Nijs, *Phys. Rev. Lett.* **49**, 405 (1982).
- [15] T. Senthil, A. Vishwanath, L. Balents, S. Sachdev, and M. P. A. Fisher, *Science* **303**, 1490 (2004).
- [16] S. Raghu, X.-L. Qi, C. Honerkamp, and S.-C. Zhang, *Phys. Rev. Lett.* **100**, 156401 (2008).
- [17] D. Pesin and L. Balents, *Nat. Phys.* **6**, 376 (2010).
- [18] L. A. Wray, S.-Y. Xu, Y. Xia, D. Hsieh, A. V. Fedorov, Y. S. Hor, R. J. Cava, A. Bansil, H. Lin, and M. Z. Hasan, *Nat. Phys.* **7**, 32 (2011).
- [19] D. Xiao, W. Zhu, Y. Ran, N. Nagaosa, and S. Okamoto, *Nat. Commun.* **2**, 596 (2011).
- [20] A. Rüegg and G. A. Fiete, *Phys. Rev. Lett.* **108**, 046401 (2012).
- [21] M. Hohenadler and F. F. Assaad, *J. Phys. Condens. Matter* **25**, 143201 (2013).
- [22] M. Kargarian and G. A. Fiete, *Phys. Rev. Lett.* **110**, 156403 (2013).
- [23] X. Deng, K. Haule, and G. Kotliar, *Phys. Rev. Lett.* **111**, 176404 (2013).
- [24] I. F. Herbut and L. Janssen, *Phys. Rev. Lett.* **113**, 106401 (2014).
- [25] J. C. Budich, B. Trauzettel, and G. Sangiovanni, *Phys. Rev. B* **87**, 235104 (2013).
- [26] A. Georges, L. de’ Medici, and J. Mravlje, *Annu. Rev. Condens. Matter Phys.* **4**, 137 (2013).
- [27] A. Georges, G. Kotliar, W. Krauth, and M. J. Rozenberg, *Rev. Mod. Phys.* **68**, 13 (1996).
- [28] J. C. Budich, R. Thomale, G. Li, M. Laubach, and S.-C. Zhang, *Phys. Rev. B* **86**, 201407(R) (2012).
- [29] N. Parragh, G. Sangiovanni, P. Hansmann, S. Hummel, K. Held, and A. Toschi, *Phys. Rev. B* **88**, 195116 (2013).
- [30] Z. Wang, X.-L. Qi, and S.-C. Zhang, *Phys. Rev. B* **85**, 165126 (2012).
- [31] Z. Wang and S.-C. Zhang, *Phys. Rev. X* **2**, 031008 (2012).
- [32] S. Rachel and K. Le Hur, *Phys. Rev. B* **82**, 075106 (2010).
- [33] M. Ezawa, Y. Tanaka, and N. Nagaosa, *Sci. Rep.* **3**, 2790 (2013).
- [34] J. C. Budich, *Phys. Rev. B* **87**, 161103(R) (2013).
- [35] V. Gurarie, *Phys. Rev. B* **83**, 085426 (2011).
- [36] B. M. Wojek, P. Dziawa, B. J. Kowalski, A. Szczerbakow, A. M. Black-Schaffer, M. H. Berntsen, T. Balasubramanian, T. Story, and O. Tjernberg, *Phys. Rev. B* **90**, 161202 (2014).
- [37] G. Borghi, M. Fabrizio, and E. Tosatti, *Phys. Rev. B* **81**, 115134 (2010).